

A Putative Insulin-like Androgenic Gland Hormone Receptor Gene Specifically Expressed in Male Chinese Shrimp

Qing Guo,^{1,2,3} Shihao Li,^{1,2} Xinjia Lv,^{1,3} Jianhai Xiang,^{1,2} Amir Sagi,⁴ Rivka Manor,⁴ and Fuhua Li^{1,2}

¹CAS Key Laboratory of Experimental Marine Biology, Institute of Oceanology, Chinese Academy of Sciences, Qingdao 266071, China; ²Laboratory for Marine Biology and Biotechnology, Qingdao National Laboratory for Marine Science and Technology, Qingdao 266237, China; ³University of Chinese Academy of Sciences, Beijing 100049, China; and ⁴Department of Life Sciences, Ben-Gurion University of the Negev, 84105 Beer-Sheva, Israel

The insulin-like androgenic gland hormone (IAG) is the key regulator in crustacean male sexual differentiation. As a secreted peptide hormone, IAG might perform its biological function through interacting with the membrane receptor. However, the receptor of IAG remains unclear. In the current study, a putative IAG receptor gene (*FclAGR*) was identified in *Fenneropenaeus chinensis*. The deduced amino acid sequence of *FclAGR* contained several conserved domains of insulin-like receptor proteins, including two L domains (L1 and L2), a cysteine-rich domain, three fibronectin III domains, a transmembrane domain, and an intracellular tyrosine kinase domain. Tissue distribution and *in situ* hybridization analysis showed that *FclAGR* was predominantly expressed in the androgenic gland and testis in male *F. chinensis*. Protein colocalization analysis in HEK293 cells showed that *FclAGR* could colocalize with both *FclAG1* and *FclAG2*, respectively. Yeast two-hybrid assay further confirmed the interactions between *FclAGR* and *FclAGs*. After a long-term silencing of *FclAGR* with double-stranded RNA, most of the germ cells in the testis were arrested at the secondary spermatocytes, whereas those in the control developed into sperm cells. The data indicated that *FclAGR* was the receptor of *FclAGs* in *F. chinensis*. The current study provides insight into the mechanism that the insulin-like signaling pathway regulates the male sexual differentiation in Decapoda crustaceans. (*Endocrinology* 159: 2173–2185, 2018)

Sex determination and sex differentiation have always been key issues in developmental biology. As an important marine group, the sex determination and sex differentiation of the crustaceans have attracted increasing attention. Crustaceans generally display sex dimorphism in growth (1). Therefore, monosex aquaculture of economic crustacean species could significantly increase the yield (2). Crustaceans have a unique endocrine regulatory system, which affects many physiological processes, such as sex differentiation (3), growth, and molting (4). The sinus gland–androgenic gland (AG)–testicular endocrine axis plays a key role in sex

differentiation of crustaceans (5). However, it is still unclear how the endocrine axis regulates the downstream pathways at the molecular level.

As one of the most important endocrine glands unique to the male crustacean, the ductless accessory gland was first discovered in the blue crab *Callinectes sapidus* (6) and then named “androgenic gland” (7). The function of AG that controls both the primary and secondary male sexual characters has been demonstrated by removing or grafting AG to opposite sexes. Implanting AG to the female could completely inhibit the vitellogenesis in *Orchestia gammarella* (8), whereas removing AG from

ISSN Online 1945-7170

Copyright © 2018 Endocrine Society

Received 21 December 2017. Accepted 15 March 2018.

First Published Online 27 March 2018

Abbreviations: AG, androgenic gland; cDNA, complementary DNA; CR, cysteine-rich; DIG, digoxigenin; dsRNA, double-stranded RNA; EGFP, enhanced green fluorescent protein; FNIII, fibronectin III; H&E, hematoxylin and eosin; IAG, insulin-like androgenic gland hormone; IGF, insulin-like growth factor; IR, insulin-like receptor; ORF, open reading frame; PCR, polymerase chain reaction; RFF, RNA-friendly fixative; RNAi, RNA interference; rRNA, ribosomal RNA.

the male individuals led to the oogenesis instead of spermatogenesis in *Armadillidium vulgare* (9, 10). Morphological masculinization in AG grafted females (11) and feminization of AG ablated males (12, 13) were also observed in decapods of crustaceans. In the crayfish *Cherax quadricarinatus*, AG ablation from the intersex individuals resulted in sex shifts in morphology (9), physiology (14), and gene transcriptions (15). Further studies showed a full feminization to produce functional females after AG ablation (16, 17).

AG functions through a protein hormone named insulin-like androgenic gland hormone (IAG; originally called androgenic gland hormone), which is secreted by AG in the male crustacean. IAG was isolated and identified as a protein consisting of a signal peptide, B chain, A chain, and C peptide, structurally belonging to the insulin superfamily (18). The first complementary DNA (cDNA) encoding an IAG precursor was reported in the terrestrial isopod *A. vulgare* (19). In decapods, the cDNA sequence of IAG gene was first reported in *C. quadricarinatus* (20), and then it was reported in different species (21–25). Silencing of IAG by double-stranded RNA (dsRNA) (26) and *in vitro* bioassay of its recombination protein (27, 28) further confirmed the function of IAG in regulating male sexual differentiation.

The insulin-like signaling pathway plays important roles in growth, metabolism, stress resistance, reproduction, and longevity in diverse organisms (29–32). Insulin-like peptides can bind with the ectodomain of insulin-like peptide receptors to initiate the downstream phosphorylation cascade (29). The insulin-like receptor (IR), as a transmembrane receptor, belongs to a subfamily of receptor tyrosine kinases (33), which is synthesized as a single chain prepro-receptor and then glycosylated, folded, and dimerized to yield the mature $\alpha_2\beta_2$ receptor. The IR includes two L domains (L1 and L2), separated by a cysteine-rich (CR) domain, three fibronectin III (FNIII) domains, one transmembrane domain, and one conserved tyrosine kinase cytoplasmic catalytic domain (34, 35).

As an insulin-like peptide hormone, IAG probably performs its biological function through interacting with IRs in crustaceans. Four IR gene sequences were identified in the draft genome of *Daphnia pulex* (36). In *Macrobrachium rosenbergii*, a full-length cDNA of an IR (MrIR) gene was reported to affect the development of spermatocytes inside the testis. This gene showed a wide distribution in different tissues of both males and females (37). In the Eastern spiny lobster, *Sagmariasus verreauxi*, an SvIR, which was mainly detected in the antennal gland of both sexes and the testes of the males, showed an interaction with SvIAG in a reporter SRE-LUC system (38). However, there is no sex-specific IR reported.

Previously, we identified two isoforms of IAG gene (*FcIAG1* and *FcIAG2*) in the penaeid shrimp *Fenneropenaeus chinensis* (39). In the current study, a potential receptor of FcIAG1 and FcIAG2 specifically expressed in the male shrimp was identified in *F. chinensis*, and its function was analyzed. The data provide evidence on understanding the molecular mechanism that IAG regulates the male sexual differentiation in crustaceans.

Materials and Methods

Animals and tissue collection

This study was approved by the Animal Care and Ethics Committee of the Institute of Oceanology, Chinese Academy of Sciences. The experimental animals received humane care in compliance with the Principles of Laboratory Animal Care developed by the National Society for Medical Research.

Ten healthy adult Chinese shrimp with a body length of 15.8 ± 0.6 cm and a body weight of 46.7 ± 1.2 g were collected and acclimated in fiberglass with air-pumped circulating sea water for 3 days before sampling. The hemolymph was collected using a syringe preloaded with an equal volume of sterilized precooled anticoagulant solution [115 mmol/L glucose, 27 mmol/L sodium citrate, 336 mmol/L NaCl, 9 mmol/L EDTA·Na₂·2H₂O (pH 7.4)]. The hemocytes were harvested from the hemolymph by centrifugation at $800 \times g$, 4°C for 10 minutes. The other tissues, including stomach, muscle, heart, lymphoid organ (Oka), gut, hepatopancreas, eyestalk, gill, ventral nerve cord, thoracic ganglia, ovary, testis and AG-related tissues (AG and part of muscle), were dissected from five female and five male individuals, respectively. All samples were immediately frozen in liquid nitrogen and stored in -80°C for RNA extraction.

Besides, testis and AG-related tissues were sampled from the male shrimp and cut into 4-mm³ pieces and fixed in RNA-friendly fixative (RFF) for 48 hours at 4°C. Then, the tissues were dehydrated with serial ethanol, cleared with serial xylene, and finally embedded in paraffin. Tissues were cut into 5- to 7- μm sections for hematoxylin and eosin (H&E) staining or *in situ* hybridization.

RNA extraction and cDNA synthesis

Total RNAs were extracted from different tissues using RNAiso Plus reagent (TaKaRa, Kyoto, Japan) according to the manufacturer's instructions. Agarose electrophoresis and NanoDrop 2000 (Thermo Fisher Scientific, Waltham, MA) were used to detect the quality and the concentration of the RNA, respectively. First-strand cDNA was synthesized using 1.5 μg of total RNA with a PrimeScript RT reagent kit (TaKaRa) for reverse transcription polymerase chain reaction (PCR). Genomic DNA was eliminated using 5 \times genomic DNA eraser buffer in the first step at 42°C, 5 minutes. cDNA was synthesized according to the following procedure: 37°C for 1 hour, and 85°C for 5 seconds. The RNAs from testes and AGs were reverse transcribed using a RevertAid first-strand cDNA synthesis kit (Thermo Fisher Scientific) for gene cloning. The program was performed as the following procedure: 45°C for 60 minutes, 25°C for 5 minutes, and 70°C for 5 minutes. The cDNA samples were stored at -80°C for further use.

Gene cloning and sequence analysis

Five pairs of primers, that is, *FcIAGR-1F/1R*, *FcIAGR-2F/2R*, *FcIAGR-3F/3R*, *FcIAGR-4F/4R*, and *FcIAGR-5F/5R* (Table 1), were designed to validate the full cDNA sequence.

PrimeStar GXL DNA polymerase (TaKaRa) was used to amplify the gene. The PCR was performed as the following procedure: 40 cycles of denaturation at 98°C for 10 seconds, annealing at 60°C for 15 seconds, and extension at 68°C for

Table 1. Primer Sequences and Corresponding Annealing Temperature of Genes

Name	Use of Primers	Sequence (5'→3')	Expected Size (bp)	Annealing Temperature (°C)
FcIAGR-1F	Gene cloning	CGACCATTCCAGGCTCTTAG	1750	60
FcIAGR-1R		CACTTTGTCCCCGTTGTAGG		
FcIAGR-2F		CACCTACAACGGGGACAAAG	874	60
FcIAGR-2R		ACATGGGCTGATACCAAGA		
FcIAGR-3F		GTCGCATCTTGGTATCAGGC	1432	60
FcIAGR-3R	GTTGGTGCGGTTCTTGTAGG			
FcIAGR-4F	Semiquantitative PCR	CCTACAAGAACCGCACCAAC	1499	60
FcIAGR-4R		CGCCCCGATAATCGTAAAAGT		
FcIAGR-5F		GGAGGACGACGACTCAGATAA	90	60
FcIAGR-5R		GTTGAAGAATGACCAAAAAGGAA		
18S-F		TATACGCTAGTGGAGCTGGAA	136	56
18S-R	GGGGAGGTAGTGACGAAAAAAT			
FcIAGR-qF	<i>In situ</i> hybridization	ACAAGAAGGCGGAGAAGAACAT	136	56
FcIAGR-qR		CCAGGTTGACGATGATGAGGT		
FcIAGR-ishF		TAATACGACTCACTATAGGG	612	60
FcIAGR-ishR	AACAGAACC GCAGACCAGAT TAATACGACTCACTATAGGGCTC GTGACAACACTGGCTTC			
FcIAG1-EGFP-F	Colocalization	CGCTCTAGCCCCGGGCGGATCCA	291	60
FcIAG1-EGFP-R		TGTACAACGTCACCGGGATTCC GGTGGCGACCGGTGGATCCCCGG AAGTACGGGTCCTCGCAAT		
FcIAG2-EGFP-F		CGCTCTAGCCCCGGGCGGATCCA	291	60
FcIAG2-EGFP-R		TGTACAACGTCACCGGGATTCC GGTGGCGACCGGTGGATCCCCGA GGTACCGGGTCCTCGCAAT		
FcIAGR-mCherry-1F		CTCGAGCTCAAGCTTCGAATTCA	1260	60
FcIAGR-mCherry-1R		TGCTCTGCCGCGTCATCGACGG GGTGGCGACCGGTGGATCCCCGG TTGGTGGCGTTGACGAGCG		
FcIAGR-mCherry-2F		CTCGAGCTCAAGCTTCGAATTCA	1665	60
FcIAGR-mCherry-2R	TGCTCTGCCGCGTCATCGACGG GGTGGCGACCGGTGGATCCCCGG TTGGTGGCGTTGACGAGCG			
FcIAG1-AD-F	Yeast two-hybrid assay	GCCATGGAGGCCAGTGAATTCTA	291	60
FcIAG1-AD-R		TAATGTAACGGGTATTCC CAGCTCGAGCTCGATGGATCCAA AATATGGATCTTCACAAT		
FcIAG2-AD-F		GCCATGGAGGCCAGTGAATTCTA	291	60
FcIAG2-AD-R		TAATGTGACAGGTATTCC CAGCTCGAGCTCGATGGATCCCCG GGACTGGATCTTCACAAT		
FcIAGR-BD-1F		TCAGAGGAGGACCTGCATATGCTC	1260	60
FcIAGR-BD-1R		TGCCGCGTCATCGACGG CCGCTGCAGGTCGACGGATCCGTT GGTGGCGTTGACGAGCG		
FcIAGR-BD-2F		TCAGAGGAGGACCTGCATATGAAG	1665	60
FcIAGR-BD-2R	GTGACGCCCTGGAGGC CCGCTGCAGGTCGACGGATCCCCC GTACCTCGCTTCGACC			
FcIAGR-dsF	RNAi	TAATACGACTCACTATAGGGAACAG	612	60
FcIAGR-dsR		AACCGCAGACCAGAT TAATACGACTCACTATAGGGCTCGTG ACAACACTGGCTTC		
EGFP-dsF		TAATACGACTCACTATAGGGCAGTGCT	289	60
EGFP-dsR		TCAGCCGCTACCC TAATACGACTCACTATAGGGAGTTCA CCTTGATGCCGTTCTT		

3 minutes. The specific products were cloned into pMD19-T vector (TaKaRa) for sequencing.

The full length of open reading frame (ORF) and deduced amino acid sequence of *FcIAGR* was analyzed using ORF finder (<https://www.ncbi.nlm.nih.gov/orffinder/>). Conserved protein domains were predicted with SMART (<http://smart.embl-heidelberg.de/>). Protein domains were analyzed with PredictProtein (<https://www.predictprotein.org/getqueries>). Multiple sequence alignment and phylogenetic analysis were performed using ClustalW and MEGA 5.2.

Semiquantitative PCR

To detect the expression levels of *FcIAGR* in different tissues, primers *FcIAGR*-qF/qR (Table 1) were designed to generate a 136-bp fragment. Semiquantitative PCR was performed using 18S ribosomal (rRNA) as an internal reference to adjust the amount of cDNA templates. Amplification was done with the following program: denaturation at 94°C for 5 minutes; 35 cycles of denaturation at 94°C for 30 seconds, annealing at 55°C for 30 seconds, and extension at 72°C for 30 seconds; final extension at 72°C for 10 minutes. The products were assessed by electrophoresis on 1.5% agarose gel.

In situ hybridization

Transcription of digoxigenin-labeled riboprobe

Primers *FcIAGR*-ishF/R with T7 promoter at the end of *FcIAGR*-ishF were designed to amplify a 612-bp fragment of *FcIAGR* as the template for the sense probe. Primers *FcIAGR*-F/ishR with T7 promoter at the end of *FcIAGR*-ishR were designed to amplify the fragment of *FcIAGR* as the template for the antisense probe. The PCR products were purified by a MiniBEST DNA fragment purification kit (TaKaRa) and assessed by electrophoresis on 1.5% agarose gel. Digoxigenin (DIG)-labeled oligonucleotide probes were synthesized through *in vitro* transcription using DIG RNA labeling mixture (Roche, Basel, Switzerland) and TranscriptAid T7 high-yield transcription kit (Thermo Fisher Scientific). After assessing the concentration and quality of synthesized RNA probes by NanoDrop 2000 (Thermo Fisher Scientific) and agarose electrophoresis, the DIG-labeled RNA probes were stored at –80°C for later use.

In situ hybridization

Hybridization was performed following general protocol of a DIG RNA labeling kit (Roche). Paraffin-embedded testes and AG-related tissues were sectioned into slices of 5 to 7 μm. These sections were deparaffinized and hydrated. After treated with proteinase K (15 μg/mL) at 37°C for 30 minutes, the slides were fixed in 4% paraformaldehyde at 4°C for 5 minutes

and rehybridizing at 37°C for 3 hours. The final concentration of both sense RNA probe and antisense RNA probe was 1 ng/μL. RNA probe was added into the hybridization solution and incubated at 56°C overnight. After overnight hybridization, the signal was visualized by the color reaction using nitroblue tetrazolium/5-bromo-4-chloro-3-indolyl phosphate stock solution (Roche) and observed through a Nikon Eclipse 80i microscope (Nikon, Tokyo, Japan).

Colocalization of FcIAGR and FcIAGs

Plasmid construction

The plasmids pEGFP-N1 and pmCherry-N1 were digested with restriction endonucleases *EcoRI* and *BamHI* to generate linearized vectors. Primers *FcIAGR*-mCherry-1F/1R, *FcIAGR*-mCherry-2F/2R and *FcIAGR*-mCherry-1F/2R were designed to amplify the nucleotide sequences that encoded the L1-CR-L2 domains (*FcIAGR*-LCL), the three FNIII domains (*FcIAGR*-FNIII), and the extracellular region of *FcIAGR* (*FcIAGR*-ER), respectively. Primers *FcIAG1*-enhanced green fluorescent protein (EGFP)-F/R and *FcIAG2*-EGFP-F/R were designed to amplify *FcIAG1* and *FcIAG2*. All primers were added with 15-bp extensions that were homologous to the relevant linearized vector ends at both ends to generate the PCR products. The gene-specific primers are listed in Table 1. The purified PCR products were inserted into the corresponding linearized vectors by setting up in-fusion cloning reaction using an In-Fusion HD cloning kit (Clontech, Mountain View, CA). The recombinant plasmids (Table 2) were transformed into Trans5α-competent cells (TransGen Biotech, Beijing, China) for sequencing. The confirmed clones were selected and cultured for plasmid extraction. Plasmids were extracted using Plasmid Mini Kit I (Omega, Lyndhurst, NJ) and stored at –80°C for use.

Cell culture and transient transfection

HEK293 cells were cultured in a 25-mL flask supplemented with 5 mL of Dulbecco's modified Eagle medium (Gibco, Waltham, MA) mixed with 10% fetal bovine serum and penicillin-streptomycin at 37°C. HEK293 cells were seeded onto a six-well plate 24 hours before transfection. Cells were transfected with Lipofectamine 3000 (Invitrogen, Waltham, MA). Combinations (Table 2), including *FcIAG1* and *FcIAGR*-LCL, *FcIAG1* and *FcIAGR*-FNIII, *FcIAG1* and *FcIAGR*-ER, *FcIAG2* and *FcIAGR*-LCL, *FcIAG2* and *FcIAGR*-FNIII, and *FcIAG2* and *FcIAGR*-ER, were used for cotransfection. pEGFP-N1 and pmCherry-N1 were used as control group. The images of the distribution patterns of *FcIAGR* and *FcIAGs* were acquired through a Nikon Eclipse Ti fluorescence microscope (Nikon) after 48 hours of culturing.

Table 2. Information of the Plasmid Construction for Colocalization and Yeast Two-Hybridization Detection

	FcIAG1	FcIAG2	FcIAG1	FcIAG2
	Colocalization		Yeast two-hybridization assay	
FcIAGR-LCL	pEGFP-FcIAG1 and pmCherry-FcIAGR-LCL	pEGFP-FcIAG2 and pmCherry-FcIAGR-LCL	pGAD-FcIAG1 and pGBK-FcIAGR-LCL	pGAD-FcIAG2 and pGBK-FcIAGR-LCL
FcIAGR-FNIII	pEGFP-FcIAG1 and pmCherry-FcIAGR-FNIII	pEGFP-FcIAG2 and pmCherry-FcIAGR-FNIII	pGAD-FcIAG1 and pGBK-FcIAGR-FNIII	pGAD-FcIAG2 and pGBK-FcIAGR-FNIII
FcIAGR-ER	pEGFP-FcIAG1 and pmCherry-FcIAGR-ER	pEGFP-FcIAG2 and pmCherry-FcIAGR-ER	pGAD-FcIAG1 and pGBK-FcIAGR-ER	pGAD-FcIAG2 and pGBK-FcIAGR-ER

Yeast two-hybrid assay

Plasmid construction

A yeast two-hybrid system was used to further prove the interaction between the FcIAGs and FcIAGR. Both plasmids, that is, pGADT7 and pGBKT7, were digested with restriction endonucleases *EcoRI* and *BamHI* to generate linearized vectors. The nucleotide sequences of B chain and A chain of FcIAG1 and FcIAG2 genes were synthesized by Sangon Biotech (Shanghai, China). Primers *FcIAGR*-BD-1F/1R, *FcIAGR*-BD-2F/2R, *FcIAGR*-BD-1F/2R, *FcIAG1*-AD-F/R, and *FcIAG2*-AD-F/R (Table 1) were used to amplify the nucleotide sequences that encoded FcIAGR-LCL, FcIAGR-FNIII, and FcIAGR-ER and synthesized FcIAGs, respectively. The procedure for the primer design and the construction of expression vectors were the same as described in "Plasmid construction" above.

Yeast transformation and galactosidase assays

The recombinant plasmids combinations as described in "Cell culture and transient transfection" above (Table 2) were cotransformed into yeast strain Y2H Gold by the lithium acetate transformation procedure according to Matchmaker protocol manual (Clontech). The pGBK-p53 and pGAD-T-antigen were used for positive control. The pGBK-Lam and pGAD-T-antigen were used for negative control. After cotransforming, the yeast transformants were coated on SD/-Leu/-Trp (DDO) plates, growing 3 to 5 days at 30°C. All clones growing on DDO were collected and cultured on SD/-Leu/-Trp/X- α -gal (DDO/X) plates for 5 to 7 days at 30°C. Blue clones were selected and

plated on SD/-Leu/-Trp/-His/-Ade/X- α -gal/Aba (QDO/X/A) plates to perform β -galactosidase activity analysis.

Preparation of dsRNA

A pair of primers with T7 promoter sequence, that is, *FcIAGR*-dsF and *FcIAGR*-dsR (Table 1), was designed to amplify a 612-bp cDNA fragment of *FcIAGR* gene. The PCR was performed as the following procedure: 40 cycles of denaturation at 98°C for 10 seconds, annealing at 60°C for 15 seconds, and extension at 68°C for 3 minutes. Primers of *EGFP*-dsF and *EGFP*-dsR with the T7 promoter sequences (Table 1) were used to clone a 289-bp DNA fragment of *EGFP* gene based on pEGFPN1 plasmid for dsRNA synthesis. The PCR program was performed as follows: one cycle of 94°C for 5 minutes; 40 cycles of 94°C for 30 seconds, 60°C for 30 seconds, and 72°C for 30 seconds; followed by one cycle of 72°C for 10 minutes. The PCR products were purified by a MiniBEST DNA fragment purification kit (TaKaRa) and used as the template for dsRNA synthesis with a TranscriptAid T7 high-yield transcription kit (Thermo Fisher Scientific). Single-strand RNA was digested by RNaseA (Thermo Fisher Scientific). Synthesized dsRNA (dsIAGR and dsEGFP) was assessed on 1.5% agarose gel, and the concentration was measured by Nanodrop 2000 (Thermo Fisher Scientific) and stored at -80°C until use.

RNA interference and quantitative real-time PCR

To optimize the silencing efficiency of dsRNA of *FcIAGR*, male Chinese shrimp at 60 days postlarval stage were chosen to optimize the dsRNA dosage. Genetic sex marker developed by

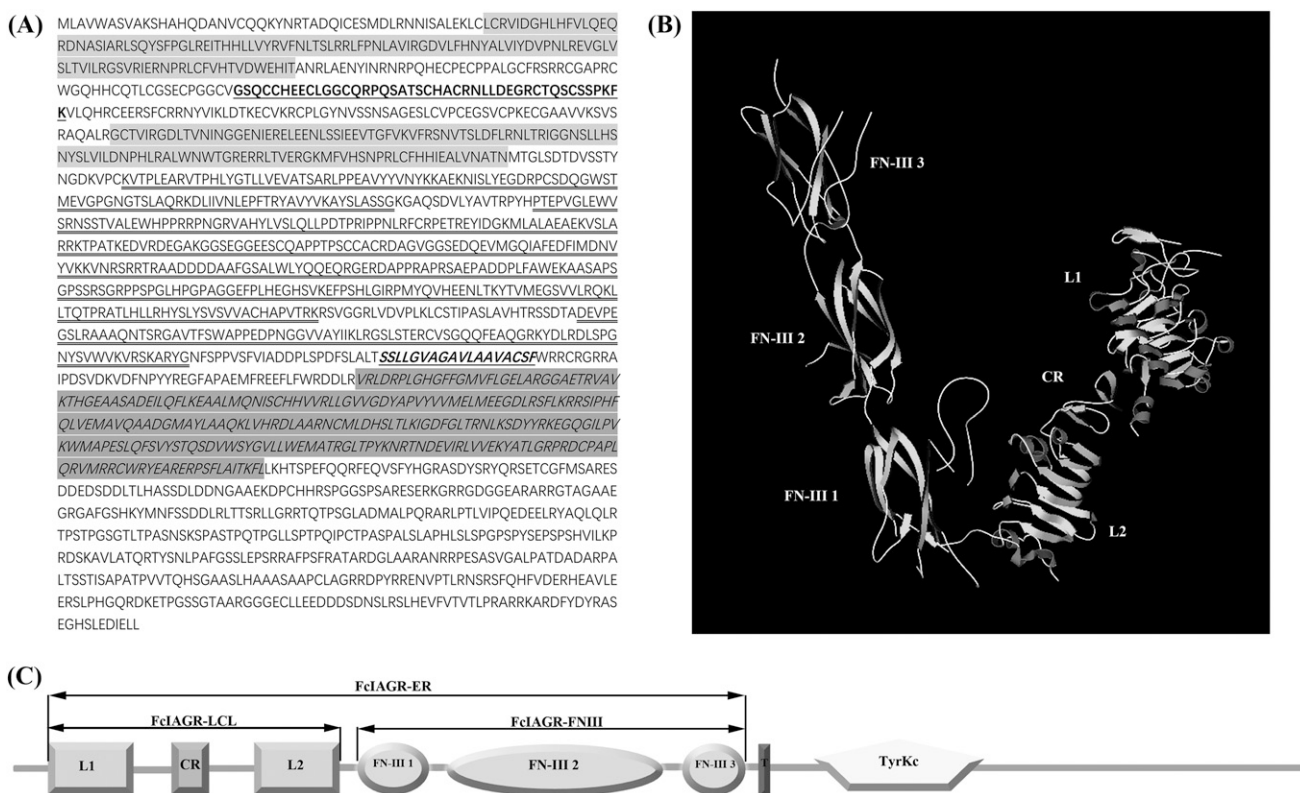


Figure 1. Deduced amino acid sequence and predicted domains of FcIAGR. (A) Two L domains (L1 and L2) are shown with a light gray box. The CR region is in bold type and underlined. Three FNIII domains are displayed with underlining. The transmembrane domain is shown as italic and underlined characters. The predicted intracellular tyrosine kinase domain is shown as italic with a dark gray box. (B) Three-dimensional model of the ectodomain of FcIAGR. (C) The schematic representation of FcIAGR with indication of L1, L2, CR, transmembrane domain (T), tyrosine kinase domain (TyrKc), FNIII, FcIAGR-LCL, FcIAGR-FNIII, and FcIAGR-ER. FNIII 1, the first FNIII domain; FNIII 2, the second FNIII domain; FNIII 3, the third FNIII domain.

our laboratory was used to identify the sex of shrimp (unpublished data), and male individuals were used for further RNA interference (RNAi) experiments. Different injection dosages, including 1 μg, 2 μg, 4 μg, 6 μg, and 8 μg, for each individual were set to detect the efficiency of RNAi.

After optimization to the dsRNA dosage for RNAi, 6 μg was chosen to inject into each shrimp. Two hundred sixty individuals at postlarval stage 60 with body length of 2.4 ± 0.3 cm were divided into two groups (control group and experimental group) for RNAi experiments. For the control group, each shrimp was injected with 6 μg of dsEGFP, and for the experimental group, each individual was injected with 6 μg of dsIAGR every 10 days. The process lasted for 60 days. AGs and testes of three individuals were sampled at 60 days after 48-hour injection with dsIAGR or dsEGFP, respectively. Total RNA extraction and cDNA synthesis was the same as described in “RNA extraction and cDNA synthesis” above.

SYBR Green–based quantitative real-time PCR was performed to detect the gene expression levels of FcIAGR. 18S rRNA was used as a reference gene. Primers FcIAGR-qF/qR and 18S-qF/qR (Table 1) were used. The melting temperature of FcIAGR-qF/qR and 18S-qF/qR was 55°C and 56°C, respectively. The PCR amplification efficiency of FcIAGR-qF/qR and 18S-qF/qR was 101.2% and 95.7%, respectively. The quantitative real-time PCR was running on an Eppendorf Mastercycler ep realplex (Eppendorf, Hamburg, Germany) using SuperReal PreMix Plus (SYBR Green) (Tiangen, Beijing, China) under the conditions as follows: denaturation at 94°C for 2 minutes; 40 cycles of 94°C for 20 seconds,

56°C for 20 seconds, and 72°C for 20 seconds. The relative expression levels of FcIAGR were calculated using the comparative cycle threshold (Ct) method with the equation 2^{-ΔΔCt}. An unpaired two-tailed t test and Tukey multiple comparison test were used for statistical analysis by GraphPad Prism software (version 5.0). A P value of <0.05 was considered statistically significant.

Histological observation on the testis of dsIAGR-injected shrimp

At the end of the RNAi experimental period, shrimp from two groups with body length of 7.1 ± 0.6 cm were collected. Testes were dissected from the animals and cut into 4-mm³ pieces and fixed in RFF for 48 hours at 4°C. After dehydration in gradient ethanol, they were embedded in paraffin as described in “Transcription of digoxigenin-labeled riboprobe” above. Paraffin-embedded AGs and testes tissues were sectioned into slices of 5 to 7 μm. The sections were then stained with H&E and observed under a Nikon Eclipse 80i microscope (Nikon).

Results

The nucleotide and deduced amino acid sequences of FcIAGR

A transcript identified as a putative IAG receptor (*FcIAGR*) using BlastX (<https://blast.ncbi.nlm.nih.gov/Blast.cgi>) was

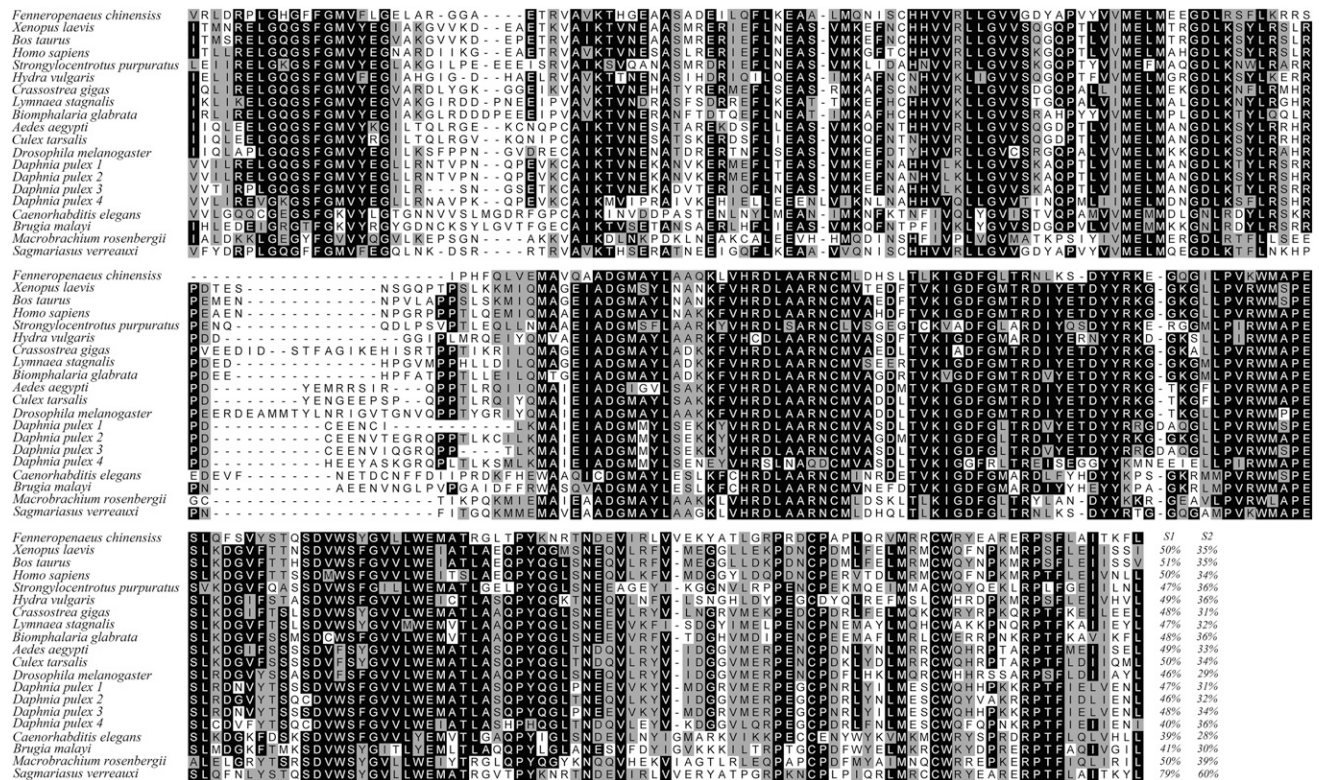


Figure 2. Multiple sequence alignment of the tyrosine kinase domain of FcIAGR with other sequences of IRs. FcIAGR and other homologous genes from species (*Caenorhabditis elegans*, AAC47715; *Brugia malayi*, AAW50597; *Strongylocentrotus purpuratus*, ABC61312; *Hydra vulgaris*, Q25197.1; *Homo sapiens*, NP_00866.1; *Xenopus laevis*, AAC12942.1; *Aedes aegypti*, AAB17094; *Culex tarsalis*, JAV35032.1; *Drosophila melanogaster*, AAC47458; *Crassostrea gigas*, CAD59674; *Biomphalaria glabrata*, AAF31166; *Lymnaea stagnalis*, CAA59353; *M. rosenbergii*, AKF17681.1; *S. verreauxi*, ANC28181.1) were used for analysis. The conserved identical residues are highlighted among the sequences with dark background, and similar residues are highlighted with different gray background. Similarity 1 (S1) showed the similarity between the tyrosine kinase domain of FcIAGR and those of other IRs. Similarity 2 (S2) showed the similarity between the whole amino acid sequence of FcIAGR and those of other IRs.

obtained from the transcriptome database of *F. chinensis* constructed in our laboratory. The transcript was confirmed by PCR amplification and sequencing. It was designated as *FcIAGR*. The ORF of *FcIAGR* (GenBank accession no. MG669585) was 5436 bp in length, encoding 1812 amino acid residues. The deduced amino acid sequence of *FcIAGR* contained the conserved domains of IR family members, including two L domains (L1 and L2) (Leu⁴⁹-Thr¹⁶⁴, Gly³³⁸-Asn⁴⁵⁴), a CR domain (Gly²²²-Lys²⁶⁵), three FNIII domains (Lys⁴⁷⁵-Gly⁵⁷⁵, Pro⁵⁹²-Lys⁸⁹⁷, Asp⁹³⁰-Gly¹⁰¹⁵), a transmembrane domain (Ser¹⁰⁴⁰-Phe¹⁰⁵⁷), and an intracellular tyrosine kinase domain (Val¹¹⁰³-Leu¹³⁵⁶) [Fig. 1(A) and 1(C)]. A three-dimensional model of the ectodomain was constructed as a “V” type [Fig. 1(B)].

Sequence similarities and classification of IR family members

Multiple alignments revealed that the tyrosine kinase domain was the most conserved region among IRs from invertebrates to vertebrates, whereas the similarities among the whole amino acid sequences of different IRs were relatively low (Fig. 2). *FcIAGR* showed the highest similarity (79%) in the tyrosine kinase domain with SvIR from *S. verreauxi*, followed by IRs from other species

with the similarities ranging from 51% to 39%. For the whole amino acid sequence, *FcIAGR* also showed the highest similarity (60%) with SvIR, followed by IRs from other species with the similarities ranging from 39% to 28% (Fig. 2). The phylogenetic analysis showed that *FcIAGR* was clustered into a separate branch with IRs from decapods *M. rosenbergii* and *S. verreauxi*. However, IRs from another crustacean, *D. pulex*, were first clustered with IRs from insects and mollusks, and then clustered together with IRs from vertebrates (Fig. 3).

Tissue distribution of *FcIAGR*

Semiquantitative PCR was performed to analyze the expression pattern of *FcIAGR* among different tissues from female and male Chinese shrimp. After 35-cycle amplifications, the transcripts of *FcIAGR* were mainly distributed in AG and testis. Weak amplification was detected in gut (Fig. 4). There was no amplification detected in other tissues.

In situ hybridization analysis was performed to localize the transcripts of *FcIAGR* in testis and AG. The results showed that *FcIAGR* transcripts were exclusively expressed in the cells of the AG, whereas they were mainly located in the spermatocytes and sperm cells in the testis (Fig. 5).

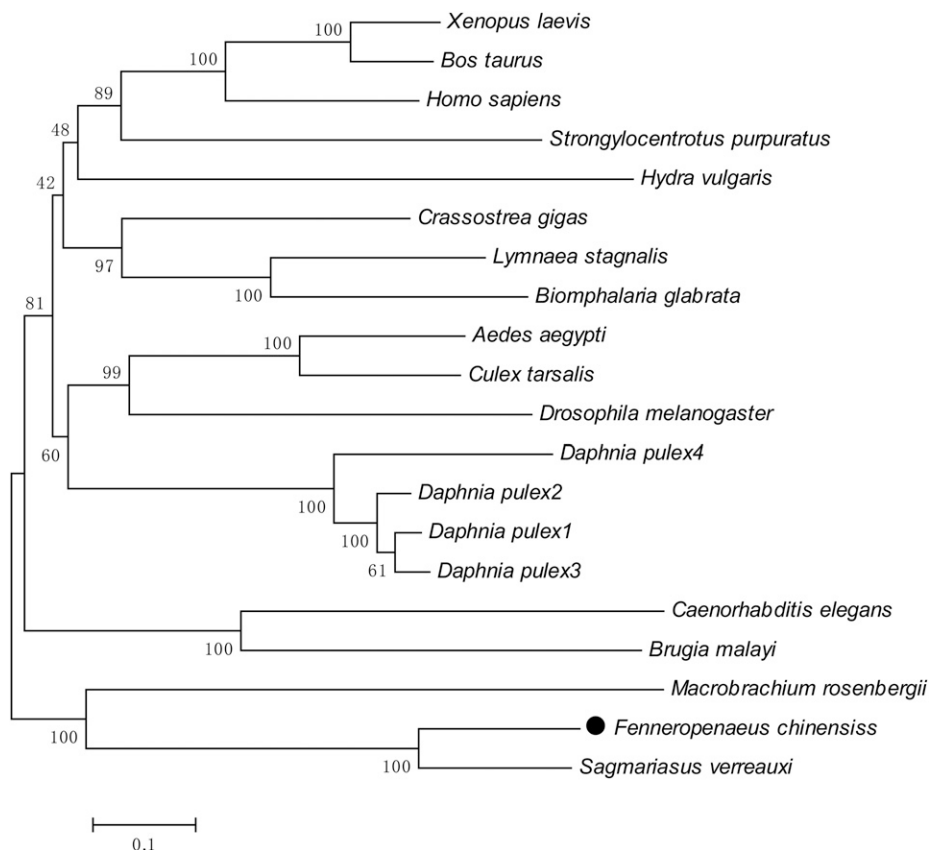


Figure 3. Phylogenetic analysis of *FcIAGR* (●) and other homologous genes from other species. Bootstraps were performed with 1000 replicates to ensure reliability. *FcIAGR* homologous genes used for phylogenetic analysis are listed in Fig. 2.

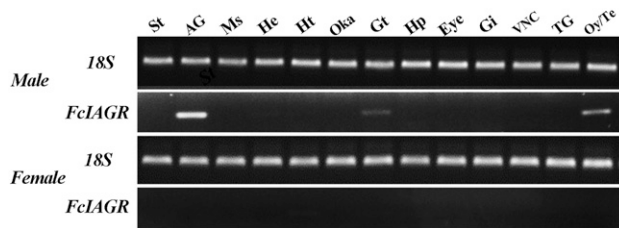


Figure 4. Expression pattern of *FcIAGR* in different tissues of *F. chinensis*. 18S rRNA gene was used as the internal reference. AG, androgenic gland related tissues; Es, eyestalk; Gi, gill; Gt, gut; Hc, hemocyte; Hp, hepatopancreas; Ht, heart; Ms, muscle; Oka, lymph organ; Ov, ovary; St, stomach; Te, testis; TG, thoracic ganglia; VNC, ventral nerve cord.

Colocalization of *FcIAGR* and *FcIAGs*

According to the tissue distribution of *FcIAGR* in male animals, we speculated that some relationships should exist in *FcIAGR* and *FcIAGs*. Therefore, we subsequently investigated the colocalization of *FcIAGR* and *FcIAGs* in HEK293 cells. In the negative control group, the green and red fluorescence signals expressed by pEGFP-N1 and pmCherry-N1 were evenly distributed in the cytoplasm of HEK293 cells (Fig. 6A), indicating that no interactions between EGFP and mCherry fluorescent proteins occurred. On the contrary, the fluorescence signals were aggregated into bright spots in the cytoplasm of HEK293 cells when they were cotransfected with the constructed pmCherry-*FcIAGR*-LCL plasmid and pEGFP-*FcIAG1*

plasmid (Fig. 6Ba–d), or pmCherry-*FcIAGR*-LCL plasmid and pEGFP-*FcIAG2* plasmid (Fig. 6Ca–d), indicating that an interaction existed for each of the two combinations. The fluorescence signals expressed by HEK293 cells that cotransfected with the constructed pmCherry-*FcIAGR*-FNIII plasmid and pEGFP-*FcIAG1* plasmid (Fig. 6Be–h) or the pmCherry-*FcIAGR*-FNIII plasmid and pEGFP-*FcIAG2* plasmid (Fig. 6Ce–h) were evenly distributed in the cytoplasm, which were the same as the result observed in the negative control group. Nevertheless, the fluorescence signals were found aggregating into bright spots in HEK293 cells that were cotransfected with constructed pmCherry-*FcIAGR*-ER plasmid and pEGFP-*FcIAG1* plasmid (Fig. 6Bi–l), or pmCherry-*FcIAGR*-ER plasmid and pEGFP-*FcIAG2* plasmid (Fig. 6Ci–l).

Interaction between *FcIAGR* and *FcIAGs*

A two-yeast hybrid assay was performed to examine whether *FcIAGR* had interaction with *FcIAGs*. In the positive control, pGBK-p53 and pGAD-T-antigen plasmids were cotransfected into yeast cells, and the reporter gene was activated and the colonies turned blue (Fig. 7, zone 1). When the yeast cells were cotransfected with plasmids expressing *FcIAGR*-LCL and *FcIAG1* (Fig. 7A, zone 2), *FcIAGR*-ER and *FcIAG1* (Fig. 7C, zone 2), *FcIAGR*-LCL and *FcIAG2* (Fig. 7D, zone 2), or *FcIAGR*-ER and *FcIAG2* (Fig. 7F, zone 2), the reporter gene was

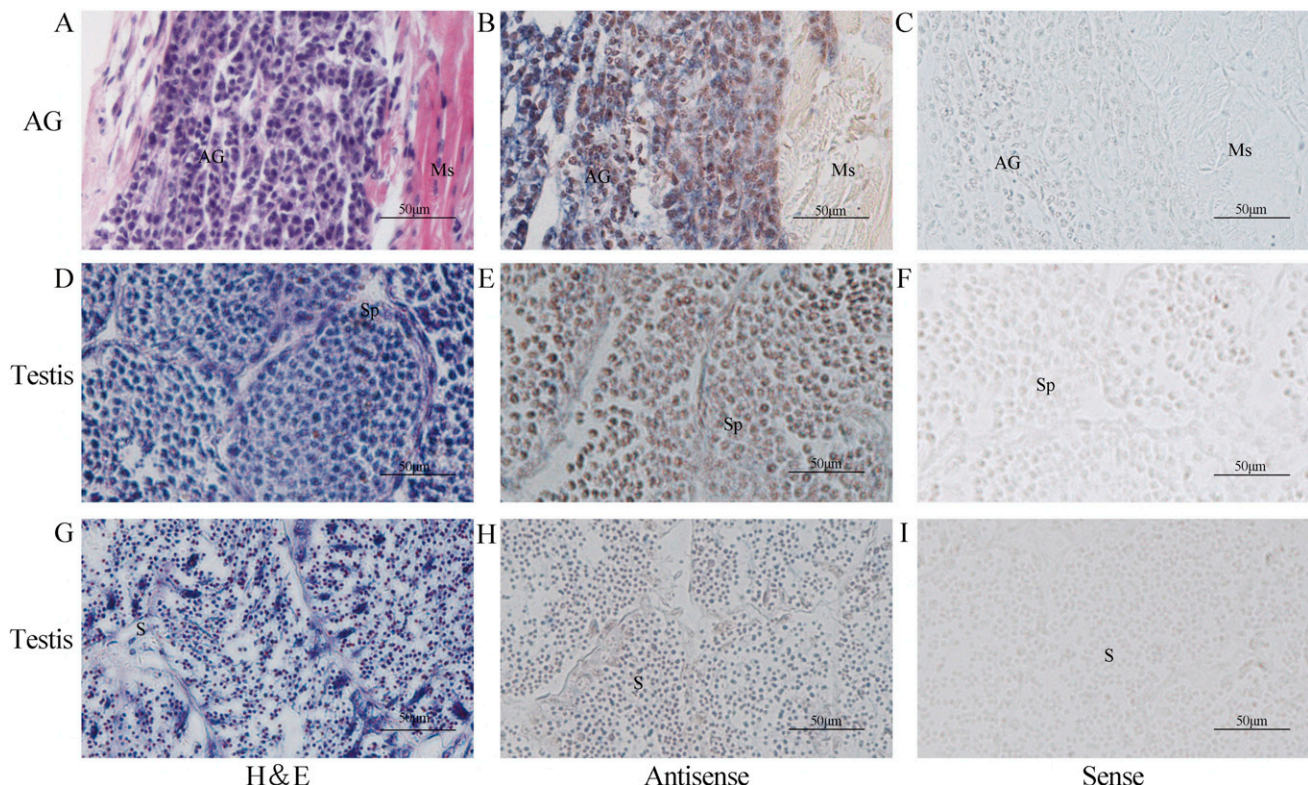


Figure 5. Localization of *FcIAGR* transcripts in the AG and testis of *F. chinensis*. (A, D, and G) H&E staining and (C, F, and I) sense probe were used as controls of (B, E, and H) the antisense probe hybridization. AG, androgenic gland; Ms, muscle; S, sperm cell; Sp, spermatocyte.

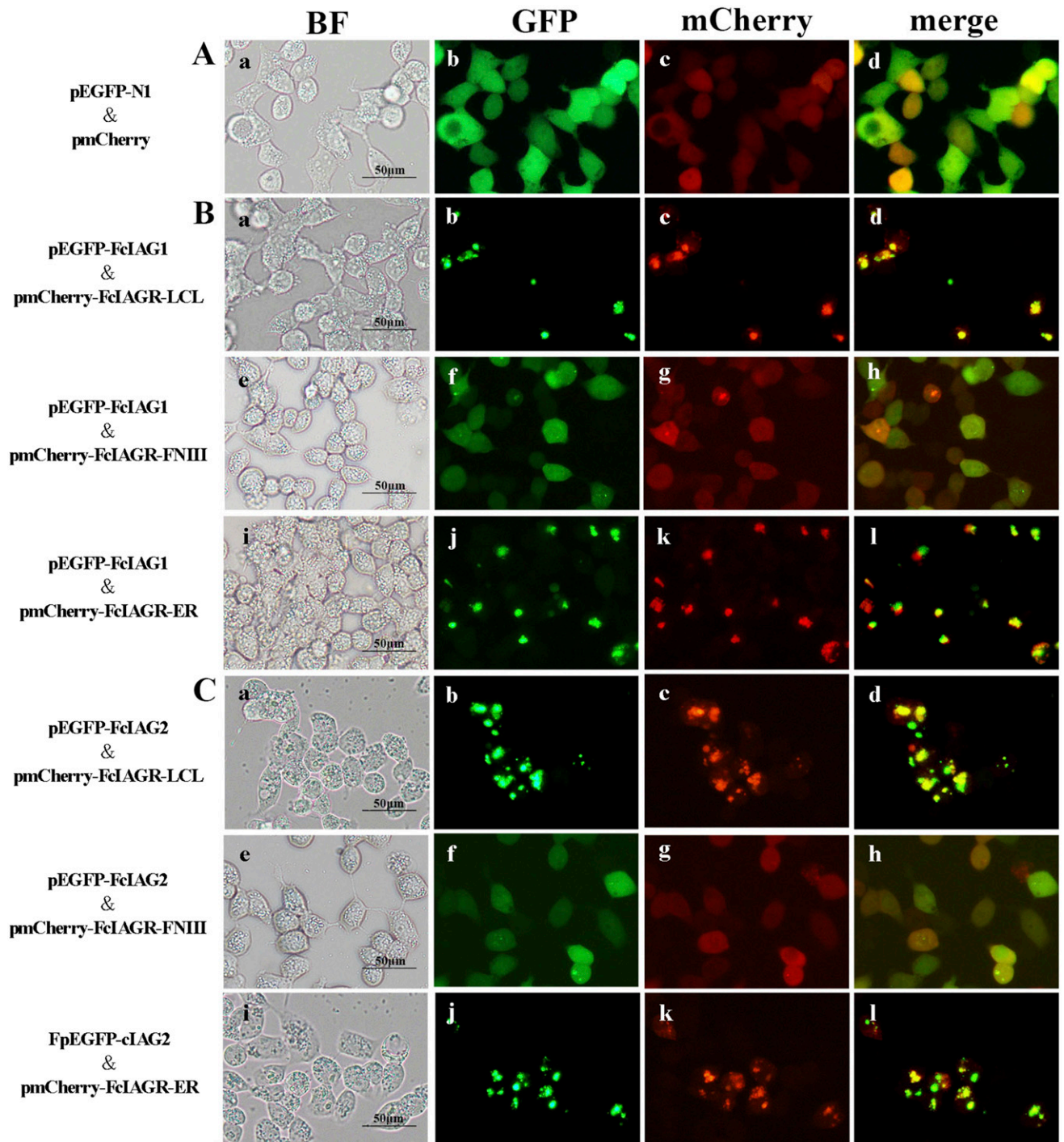


Figure 6. Colocalization of FcIAGR and FcIAGs. HEK293 cells were transfected with a combination of the indicated plasmids. (A) pEGFP-N1 and pmCherry-N1. (B) pEGFP-FcIAG1 and pmCherry-FcIAGR. (C) pEGFP-FcIAG2 and pmCherry-FcIAGR. The observation fields are displayed as follows: (a), (e), and (i) were observed under bright field; (b), (f), and (j) were excited by blue light; (c), (g), and (k) were excited by green light; (d), (h), and (l) were merged by (b) plus (c), (f) plus (g), and (j) plus (k), respectively.

activated and the colonies turned blue. When the yeast cells were cotransfected with plasmids expressing FcIAGR-FNIII and FcIAG1 (Fig. 7B, zone 2) or FcIAGR-FNIII and FcIAG2 (Fig. 7E, zone 2), the reporter gene could not be activated. No expression of the reporter gene was found in self-activation groups (Fig. 7, zones 3 and 4) and negative groups (Fig. 7, zone 5).

Silencing of FcIAGR arrested testis development

The silencing efficiency of dsIAGR depended on the injection dosages of dsRNA. The expression levels of *FcIAGR* gradually decreased when the dosage of dsIAGR increased. The expression level of *FcIAGR* in 6 μg of dsIAGR-injected individuals showed an extremely significant decrease compared with that in the control group

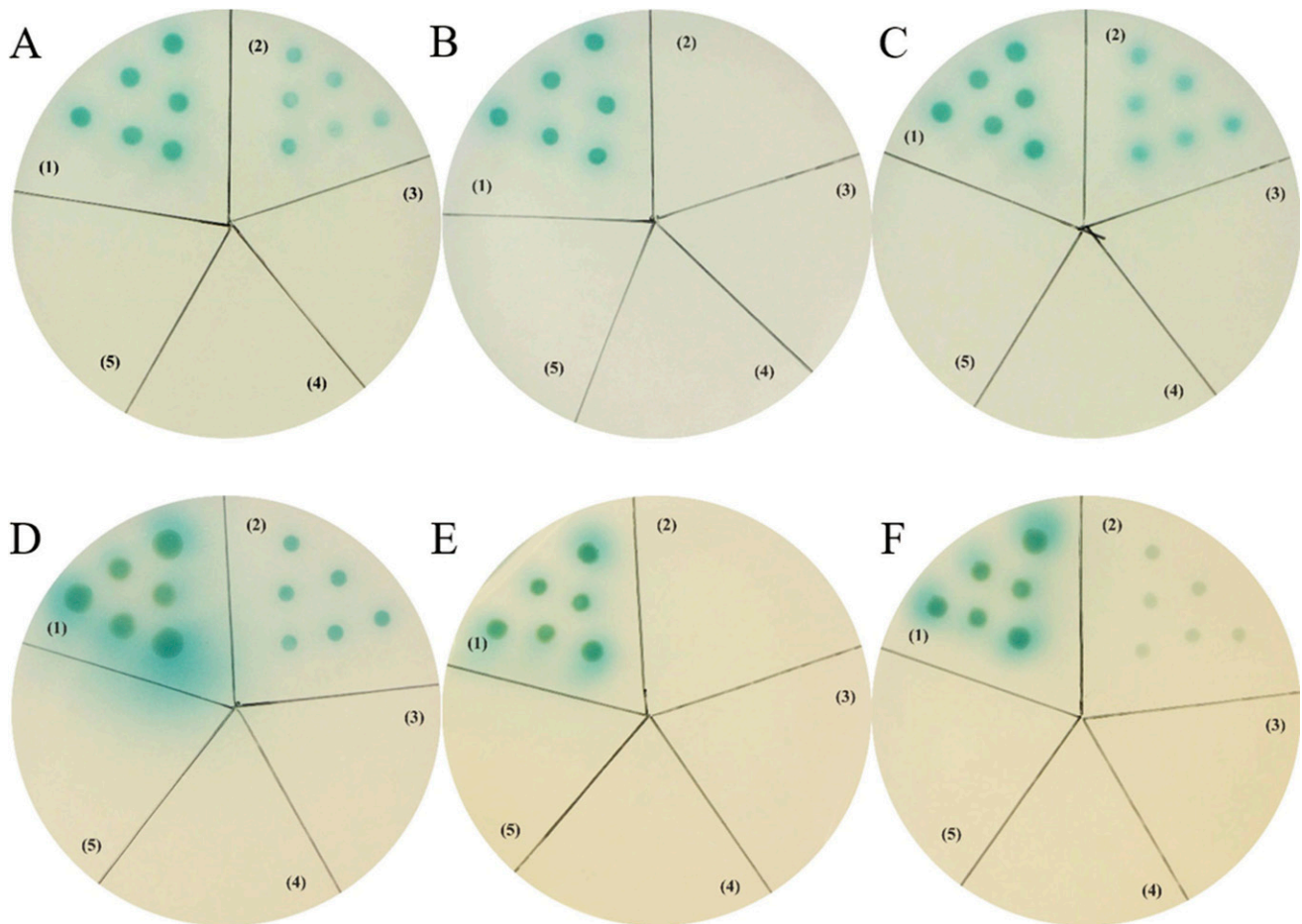


Figure 7. Yeast two-hybrid assay. Yeast cells were transformed with a combination of the indicated plasmids (1). (A–F) pGBK-p53 and pGAD-T-antigen for positive control (2). (A) pGAD-FcIAG1 and pGBK-FcIAGR-LCL plasmids. (B) pGAD-FcIAG1 and pGBK-FcIAGR-FNIII plasmids. (C) pGAD-FcIAG1 and pGBK-FcIAGR-ER plasmids. (D) pGAD-FcIAG2 and pGBK-FcIAGR-LCL plasmids. (E) pGAD-FcIAG2 and pGBK-FcIAGR-FNIII plasmids. (F) pGAD-FcIAG2 and pGBK-FcIAGR-ER plasmids (3). (A–C) pGAD-FcIAG1 and pGBK-p53 plasmids. (D–F) pGAD-FcIAG2 and pGBK-p53 plasmids (4). (A and D) pGAD-T-antigen and pGBK-FcIAGR-LCL plasmids. (B and E) pGAD-T-antigen and pGBK-FcIAGR-FNIII plasmids. (C and F) pGAD-T-antigen and pGBK-FcIAGR-ER plasmids (5). (A–F) pGBK-Lam and pGAD-T-antigen for negative control.

(Fig. 8A). After long-term RNAi experiment, 6 μg of dsIAGR significantly inhibited the expression levels of *FcIAGR* in AG and testis (Fig. 8B).

Through histological observation on the testis of shrimp with *FcIAGR* interference and those from the control group, we found that the testes from the dsEGFP-injected group showed active spermatogenesis, with highly abundant mature sperm cells in seminiferous tubules (Fig. 9A), whereas an arrest of spermatogenesis existed in the testes of shrimp with dsIAGR interference, and the secondary spermatocytes mainly existed in most seminiferous tubules of the testis (Fig. 9B).

Discussion

In crustaceans, IAG regulates male sexual differentiation. Identification of the receptor for IAG is very important for illustrating the sex differentiation mechanism in crustaceans. In the current study, a putative IAG receptor gene, termed *FcIAGR*, was isolated and characterized

from the Chinese shrimp *F. chinensis*. As a member of evolutionarily conserved IR family, *FcIAGR* contained several conserved domains of IRs (40), including two L domains, one CR domain, three FNIII domains, and one intracellular tyrosine kinase domain. The predicted three-dimensional model of the ectodomain of *FcIAGR* was similar to that of the IR in humans, like an inverted “V” (41). The phylogenetic analysis results showed that *FcIAGR* was clustered into a separate branch with IRs from decapods *M. rosenbergii* and *S. verreauxi*. However, their relationship was far from IRs in other arthropods and mollusks, which were finally constituted in a large group with IRs from vertebrates. These results indicated that *FcIAGR* might have similar biological function with SvIR and MrIR, which might be different from classical IR function.

Although two IRs (MrIR and SvIR) in decapod crustaceans *M. rosenbergii* and *S. verreauxi* have been reported to be possible IAG receptors, they showed wide distribution patterns in both sexes (37, 38). High

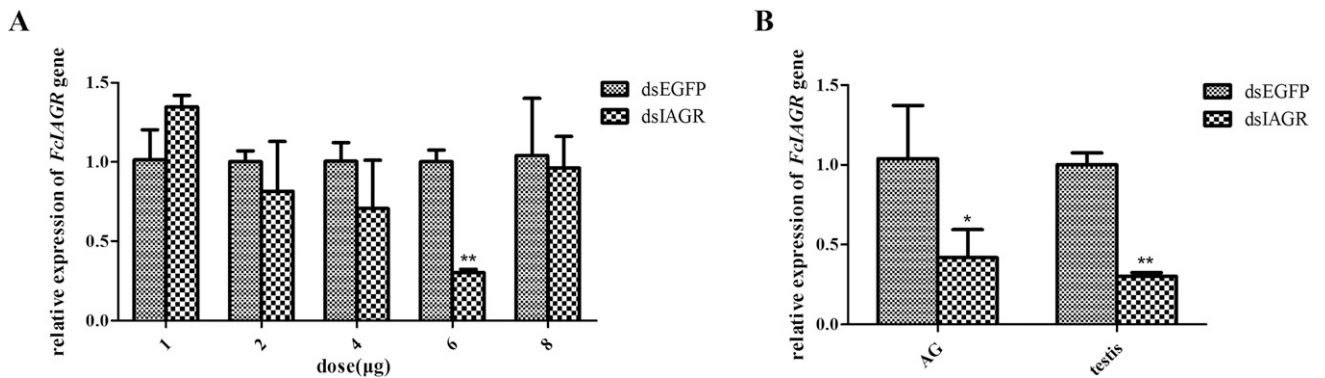


Figure 8. Expression level of *FcIAGR* after gene silencing. (A) The silencing efficiency of *FcIAGR* injected with different dosages of dsRNA. (B) Levels of *FcIAGR* transcripts in AG and testis at the end of long-term RNAi experiment. dsEGFP indicates injected with dsEGFP; dsIAGR indicates injected with dsIAGR. Significant differences of the gene expression levels between two treatments are shown as * $P < 0.05$ and ** $P < 0.01$.

expressions of *MrIR* were detected in the green gland of both sexes and the ovaries of females, whereas low expressions were detected in the head ganglia and thoracic ganglia of both sexes and the AG of male *M. rosenbergii* (37). *SvIR* was dominantly expressed in the antennal gland of both sexes and the testis of male *S. verreauxi* (38). Different from *MrIR* and *SvIR*, *FcIAGR* showed a male-specific expression pattern, which was mainly expressed in AG and testis of *F. chinensis*. The distribution pattern of *FcIAGR* gave us a clue that it was more possible to be involved in the specific function in males, especially related to AG and testis. The high expression levels of *FcIAGR* in testis might indicate that testis was a target tissue for *IAG* function. Besides, a low expression of *FcIAGR* in the gut of male rather than female shrimp might be related to the appearance of appendix masculine (16) and agonistic behavior of male individuals (42).

The insulin-like signaling pathway is directly activated by insulin-like peptides binding to their receptors. Investigating the reaction between the extracellular region of *FcIAGR* and *FcIAGs* can help establish whether *FcIAGR* functioned as the receptor of *FcIAGs*. The binding site was supposed to be located in the L1-CR-L2 domains rather than the three FNIII domains of the

ectodomain of *FcIAGR*. This was because *FcIAGR*-LCL and *FcIAGR*-ER could colocalize with both *FcIAG1* and *FcIAG2* in the HEK293 cells. However, *FcIAGR*-FNIII was not involved in the ligand–receptor binding process. Under a yeast two-hybrid assay, *FcIAGR*-LCL and *FcIAGR*-ER could also interact with *FcIAGs*. The interaction between *FcIAGR* and *FcIAGs* followed the classical binding manner of insulin to its receptor, in which insulin bound to the L1 domain and C terminus of the CR domain of its receptor (43).

In *C. quadricarinatus* and *M. rosenbergii*, *IAG* silencing could lead to the hypertrophied AG, which suggested that *IAG* might regulate its own secretion by feedback inhibition (26, 44). Expression of *FcIAGR* in both AG and testis of *F. chinensis* suggested that *FcIAGR* might participate in the feedback regulation of *FcIAGs* secretion. Different insulin-like peptides, such as insulin, insulin-like growth factor (IGF)-1, and IGF-2, bind to the receptor IGF-1R with different affinities when playing their molecular functions (45). In *F. chinensis*, the AG was the main tissue for the expression of two kinds of *FcIAG* transcripts, but they displayed different expression profiles throughout the developmental stages (23). The two *FcIAGs* could both interact with one receptor,

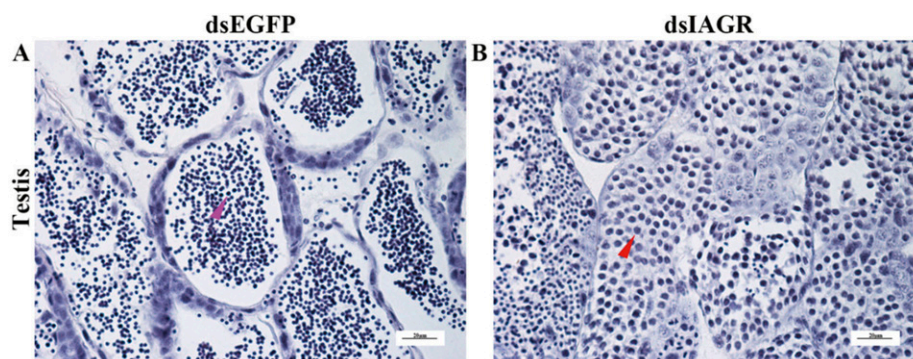


Figure 9. Effect of *FcIAGR* silencing on testis development of *F. chinensis*. H&E-stained cross-sections used for structure description. (A) Testes of dsEGFP-injected individuals show seminiferous tubules filled with mature sperm cells (pink arrowhead). (B) Testes of dsIAGR-injected animals were arrested into the secondary spermatocytes (red arrowhead). The scale bars show 20 μm .

FcIAGR, indicating that there might be a competitive regulation between FcIAG1 and FcIAG2 when they bound to the receptor.

Functional studies of *IAG* genes showed their roles in testis development and spermatogenesis. In *M. rosenbergii*, sperm was absent in either the sperm ducts or testis after silencing of *MrIAG* with dsRNA (26). In *C. quadricarinatus*, testicular degeneration and the absence of sperm in sperm duct were observed after *IAG* silencing (44). Similar results were found after silencing of the putative receptor gene *MrIR* in *M. rosenbergii*. Less sperm and more secondary spermatocytes were generated in the sperm duct after *MrIR* silencing (44). Silencing of *FcIAGR* also led to developmental arrest of spermatogenesis. After silencing of *FcIAGR*, most of the seminiferous lobes filled with secondary spermatocytes rather than sperm in the control group. *FcIAGR* might be indispensable for the spermatogenesis process from secondary spermatocytes to sperm because *FcIAGR* was widely expressed in the primary spermatocytes, secondary spermatocytes, and sperm. In vertebrates, the vital role of the family of insulin-like family factors in sex determination, testis differentiation, and reproductive function has been demonstrated (46). In mice, embryos failed to develop testis without IR and IGF-1R (47). This evidence suggested that insulin-like peptides and their receptors might have functions in male sexual differentiation. Considering that FcIAGR showed a low sequence similarity with reported IRs and presented a male-specific expression pattern rather than expression in both sexes similar to *MrIR* (37) and *SvIR* (38), FcIAGR might be the specific receptor for IAG function.

In conclusion, the current study identified and characterized a putative IAG receptor FcIAGR, which was mainly expressed in AG and testis. FcIAGR possessed the conserved domains of receptor tyrosine kinases, belonging to the IR family. Colocalization and a yeast two-hybridization assay confirmed that FcIAGR could interact with FcIAG1 and FcIAG2. The result of *FcIAGR* silencing demonstrated its function in regulating spermatogenesis. Future studies will focus on the regulation of male sexual differentiation of the *FcIAGR* gene. Additionally, structure study and chemical ligand isolation of FcIAGR protein will also be carried out to develop new sex control technology.

Acknowledgments

Financial Support: This work was supported by National Natural Science Foundation of China Grants 31461143007 (to F.L.) and 31302171 (to S.L.) and the Blue Life Breakthrough Program of LMBB (Grant MS2017NO04 to F.L.) of Qingdao National Laboratory for Marine Science and Technology.

Correspondence: Shihao Li, PhD, or Fuhua Li, PhD, Key Laboratory of Experimental Marine Biology, Institute of Oceanology, Chinese Academy of Sciences, 7 Nanhai Road, Qingdao 266071, China. E-mail: lishihao@qdio.ac.cn or fhli@qdio.ac.cn.

Disclosure Summary: The authors have nothing to disclose.

References

- Hartnoll RG. Growth. In: Bliss DE, ed. *The Biology of Crustacea, Embryology, Morphology and Genetics*. New York, NY: Academic Press; 1982:111–196.
- Sagi A, Raanan Z, Cohen D, Wax Y. Production of *Macrobrachium rosenbergii* in monosex populations: yield characteristics under intensive monoculture conditions in cages. *Aquaculture*. 1986; 51(3–4):265–275.
- Hasegawa Y, Hirose E, Katakura Y. Hormonal control of sexual differentiation and reproduction in Crustacea. *Am Zool*. 1993; 33(3):403–411.
- Abramowitz RK, Abramowitz AA. Moulting, growth, and survival after eyestalk removal in *Uca pugnator*. *Biol Bull*. 1940;78(2): 179–188.
- Khalaila I, Manor R, Weil S, Granot Y, Keller R, Sagi A. The eyestalk-androgenic gland-testis endocrine axis in the crayfish *Cherax quadricarinatus*. *Gen Comp Endocrinol*. 2002;127(2): 147–156.
- Cronin LE. Anatomy and histology of the male reproductive system of *Callinectes sapidus* Rathbun. *J Morphol*. 1947;81(2):209–239.
- Charniaux-Cotton H. Le déterminisme hormonal des caractères sexuels d'*Orchestia gammarella* (Crustacé: Amphipode). *C R Acad Sci Paris*. 1955;240(13):1487–1489.
- Charniaux-Cotton H. *Croissance, Régénération et Déterminisme Endocrinien des Caractères Sexuels Secondaires d'Orchestia gammarella (Pallas) Crustacé Amphipode*. Paris, France: Masson; 1957.
- Abdu U, Davis C, Khalaila I, Sagi A. The vitellogenin cDNA of *Cherax quadricarinatus* encodes a lipoprotein with calcium binding ability, and its expression is induced following the removal of the androgenic gland in a sexually plastic system. *Gen Comp Endocrinol*. 2002;127(3):263–272.
- Suzuki S, Yamasaki K. Sexual bipotentiality of developing ovaries in the terrestrial isopod *Armadillidium vulgare* (Malacostraca, Crustacea). *Gen Comp Endocrinol*. 1997;107(1):136–146.
- Nagamine C, Knight AW. Masculinization of female crayfish, *Procambarus clarki* (Girard). *Int J Invertebr Reprod Dev*. 1987; 11(1):77–87.
- Nagamine C, Knight AW, Maggenti A, Paxman G. Effects of androgenic gland ablation on male primary and secondary sexual characteristics in the Malaysian prawn, *Macrobrachium rosenbergii* (de Man) (Decapoda, Palaemonidae), with first evidence of induced feminization in a nonhermaphroditic decapod. *Gen Comp Endocrinol*. 1980;41(4):423–441.
- Sagi A, Cohen D, Milner Y. Effect of androgenic gland ablation on morphotypic differentiation and sexual characteristics of male freshwater prawns, *Macrobrachium rosenbergii*. *Gen Comp Endocrinol*. 1990;77(1):15–22.
- Barki A, Karplus I, Manor R, Sagi A. Intersexuality and behavior in crayfish: the de-masculinization effects of androgenic gland ablation. *Horm Behav*. 2006;50(2):322–331.
- Sagi A, Manor R, Segall C, Khalaila I. On intersexuality in the crayfish *Cherax quadricarinatus*: an inducible sexual plasticity model. *Invertebr Reprod Dev*. 2002;41(1–3):27–33.
- Sagi A, Snir E, Khalaila I. Sexual differentiation in decapod crustaceans: role of the androgenic gland. *Invertebr Reprod Dev*. 1997; 31(1–3):55–61.

17. Suzuki S, Yamasaki K. Sex-reversal of male *Armadillidium vulgare* (Isopoda, Malacostraca, Crustacea) following andrectomy and partial gonadectomy. *Gen Comp Endocrinol*. 1991;83(3):375–378.
18. Okuno A, Hasegawa Y, Nagasawa H. Purification and properties of androgenic gland hormone from the terrestrial isopod *Armadillidium vulgare*. *Zool Sci*. 1997;14(5):837–842.
19. Okuno A, Hasegawa Y, Ohira T, Katakura Y, Nagasawa H. Characterization and cDNA cloning of androgenic gland hormone of the terrestrial isopod *Armadillidium vulgare*. *Biochem Biophys Res Commun*. 1999;264(2):419–423.
20. Manor R, Weil S, Oren S, Glazer L, Aflalo ED, Ventura T, Chalifa-Caspi V, Lapidot M, Sagi A. Insulin and gender: an insulin-like gene expressed exclusively in the androgenic gland of the male crayfish. *Gen Comp Endocrinol*. 2007;150(2):326–336.
21. Banzai K, Ishizaka N, Asahina K, Suitoh K, Izumi S, Ohira T. Molecular cloning of a cDNA encoding insulin-like androgenic gland factor from the kuruma prawn *Marsupenaeus japonicus* and analysis of its expression. *Fish Sci*. 2011;77(3):329–335.
22. Chung JS, Manor R, Sagi A. Cloning of an insulin-like androgenic gland factor (IAG) from the blue crab, *Callinectes sapidus*: implications for eyestalk regulation of IAG expression. *Gen Comp Endocrinol*. 2011;173(1):4–10.
23. Li S, Li F, Sun Z, Xiang J. Two spliced variants of insulin-like androgenic gland hormone gene in the Chinese shrimp, *Fenneropenaeus chinensis*. *Gen Comp Endocrinol*. 2012;177(2):246–255.
24. Ma KY, Lin JY, Guo SZ, Chen Y, Li JL, Qiu GF. Molecular characterization and expression analysis of an insulin-like gene from the androgenic gland of the oriental river prawn, *Macrobrachium nipponense*. *Gen Comp Endocrinol*. 2013;185:90–96.
25. Zhang YQ, Qiao K, Wang SP, Peng H, Shan ZG, Wang KJ. Molecular identification of a new androgenic gland-specific insulin-like gene from the mud crab, *Scylla paramamosain*. *Aquaculture*. 2014;433:325–334.
26. Ventura T, Manor R, Aflalo ED, Weil S, Raviv S, Glazer L, Sagi A. Temporal silencing of an androgenic gland-specific insulin-like gene affecting phenotypical gender differences and spermatogenesis. *Endocrinology*. 2009;150(3):1278–1286.
27. Katayama H, Kubota N, Hojo H, Okada A, Kotaka S, Tsutsui N, Ohira T. Direct evidence for the function of crustacean insulin-like androgenic gland factor (IAG): total chemical synthesis of IAG. *Bioorg Med Chem*. 2014;22(21):5783–5789.
28. Okuno A, Hasegawa Y, Nishiyama M, Ohira T, Ko R, Kurihara M, Matsumoto S, Nagasawa H. Preparation of an active recombinant peptide of crustacean androgenic gland hormone. *Peptides*. 2002;23(3):567–572.
29. Holzenberger M, Dupont J, Ducos B, Leneuve P, Géloën A, Even PC, Cervera P, Le Bouc Y. IGF-1 receptor regulates lifespan and resistance to oxidative stress in mice. *Nature*. 2003;421(6919):182–187.
30. Nässel DR, Winther AME. *Drosophila* neuropeptides in regulation of physiology and behavior. *Prog Neurobiol*. 2010;92(1):42–104.
31. Saltiel AR, Kahn CR. Insulin signalling and the regulation of glucose and lipid metabolism. *Nature*. 2001;414(6865):799–806.
32. Teleman AA. Molecular mechanisms of metabolic regulation by insulin in *Drosophila*. *Biochem J*. 2009;425(1):13–26.
33. Ebina Y, Ellis L, Jarnagin K, Edery M, Graf L, Clauser E, Ou JH, Masiarz F, Kan YW, Goldfine ID, Roth RA, Rutter WJ. The human insulin receptor cDNA: the structural basis for hormone-activated transmembrane signalling. *Cell*. 1985;40(4):747–758.
34. Ward CW, Hoyne PA, Flegg RH. Insulin and epidermal growth factor receptors contain the cysteine repeat motif found in the tumor necrosis factor receptor. *Proteins*. 1995;22(2):141–153.
35. Yamaguchi T, Fernandez R, Roth RA. Comparison of the signaling abilities of the *Drosophila* and human insulin receptors in mammalian cells. *Biochemistry*. 1995;34(15):4962–4968.
36. Boucher P, Ditlecadet D, Dubé C, Dufresne F. Unusual duplication of the insulin-like receptor in the crustacean *Daphnia pulex*. *BMC Evol Biol*. 2010;10(1):305.
37. Sharabi O, Manor R, Weil S, Aflalo ED, Lezer Y, Levy T, Aizen J, Ventura T, Mather PB, Khalaila I, Sagi A. Identification and characterization of an insulin-like receptor involved in crustacean reproduction. *Endocrinology*. 2016;157(2):928–941.
38. Aizen J, Chandler JC, Fitzgibbon QP, Sagi A, Battaglene SC, Elizur A, Ventura T. Production of recombinant insulin-like androgenic gland hormones from three decapod species: in vitro testicular phosphorylation and activation of a newly identified tyrosine kinase receptor from the Eastern spiny lobster, *Sagmariasus verreauxi*. *Gen Comp Endocrinol*. 2016;229:8–18.
39. Li S, Zhang X, Sun Z, Li F, Xiang J. Transcriptome analysis on Chinese shrimp *Fenneropenaeus chinensis* during WSSV acute infection. *PLoS One*. 2013;8(3):e58627.
40. Adams TE, Epa VC, Garrett TPJ, Ward CW. Structure and function of the type 1 insulin-like growth factor receptor. *Cell Mol Life Sci*. 2000;57(7):1050–1093.
41. Ward CW, Lawrence MC, Streltsov VA, Adams TE, McKern NM. The insulin and EGF receptor structures: new insights into ligand-induced receptor activation. *Trends Biochem Sci*. 2007;32(3):129–137.
42. Barki A, Karplus I, Goren M. The agonistic behaviour of the three male morphotypes of the freshwater prawn *Macrobrachium rosenbergii* (Crustacea, Palaemonidae). *Behaviour*. 1991;116(3):252–276.
43. Whittaker J, Groth AV, Mynarcik DC, Pluzek L, Gadsbøll VL, Whittaker LJ. Alanine scanning mutagenesis of a type 1 insulin-like growth factor receptor ligand binding site. *J Biol Chem*. 2001;276(47):43980–43986.
44. Rosen O, Manor R, Weil S, Gafni O, Linial A, Aflalo ED, Ventura T, Sagi A. A sexual shift induced by silencing of a single insulin-like gene in crayfish: ovarian upregulation and testicular degeneration. *PLoS One*. 2010;5(12):e15281.
45. Nakayama Y, Yamamoto T, Abé SI. IGF-I, IGF-II and insulin promote differentiation of spermatogonia to primary spermatocytes in organ culture of newt testes. *Int J Dev Biol*. 1999;43(4):343–347.
46. Griffith RJ, Bianda V, Nef S. The emerging role of insulin-like growth factors in testis development and function. *Basic Clin Androl*. 2014;24(1):12.
47. Pitetti JL, Calvel P, Romero Y, Conne B, Truong V, Papaioannou MD, Schaad O, Docquier M, Herrera PL, Wilhelm D, Nef S. Insulin and IGF1 receptors are essential for XX and XY gonadal differentiation and adrenal development in mice. *PLoS Genet*. 2013;9(1):e1003160.